



## 3D QSAR study of Fluoroquinolone Derivatives as DNA Gyrase Inhibitors

Author

**Kavan. M. Jani**

Institute of Pharmacy, Nirma University, India

Email: [kavanjani25@gmail.com](mailto:kavanjani25@gmail.com)

### Abstract

*Tuberculosis is one of the major challenges around globe caused by Mycobacterium Tuberculosis. As per WHO, the rate of disease increases by 0.4% per year. DNA Gyrase being a potent target, a promising tool for the treatment of tuberculosis. Amongst all the moeity used for study, fluoroquinolone plays a key role in drug discovery and development. In order to know the structural requirements of the respective target, three-dimensional quantitative structure activity relationship (3D-QSAR) was performed on fluoroquinolone series. CoMFA and CoMSIA techniques were used to examine the structural requirements of DNA Gyrase inhibitors. The developed models indicates the high cross-validation co-efficient ( $q^2$ ) of 0.644 and 0.646 and non-cross validated co-efficient ( $r^2$ ) of 0.985 and 0.983 respectively. The validation of predictive ability of the models were carried out using external validation of predictive factor ( $r^2_{pred}$ ) of 0.685 and 0.732 respectively. These signify that the model possess high statistical reliability and good predictive power. The 3D contour maps were generated from CoMFA and CoMSIA models. Based on the, contour maps generated, the important structural features of DNA Gyrase inhibitors, with potentially higher predicted activity can be helpful for designing of new molecules. Consequently, the results obtained may provide important information in further augmentation of fluoroquinolone derivatives as DNA Gyrase inhibitors.*

**Keywords:** DNA Gyrase, CoMFA, CoMSIA, Fluoroquinolone.

### Introduction

Tuberculosis caused by Mycobacterium bacterium tuberculosis, is spreading at a higher speed around the globe and has become a major concern. The half of the world's population is affected by tuberculosis. As a result, 95% of mortality rate is reported in developing countries<sup>[1]</sup>. In spite of the fact; numerous classes of anti-microbials have been developed for the treatment of tuberculosis. The lengthy treatment regimens required for therapy can result into poor patients compliance and rapid drug-resistant strains<sup>[2]</sup>. A few of the drugs like ethambutol, cycloserine, isoniazid, rifampicin and pyrazinamide are considered to be

a successful anti-TB regimens. Here, ofloxacin and ciprofloxacin have a bacteriostatic anti-mycobacterial action but a few modern fluoroquinolones such as sparfloxacin and moxifloxacin possess high bactericidal action against M.TB. Therefore, new agents are not only helpful in shortening the time span of therapy but also has given noteworthy success in targets like macrolides, tetracyclines, cephalosporins, and quinolones<sup>[3,4]</sup>.

In this context, bacterial DNA Gyrase, a type II DNA topoisomerase being a promising target for anti-bacterial chemotherapy<sup>[4]</sup>. Fluoroquinolones are wide range anti-bacterial agents that acts by

expanding levels of DNA, strand breaks produced by type II topoisomerases<sup>[5]</sup>. It also applies its effective anti-bacterial action by interacting with DNA Gyrase and DNA topoisomerase. It also possesses in-vivo and in-vitro anti-mycobacterial activity. Fluoroquinolones are commonly endorsed for community procured pneumonia that is later diagnosed as pulmonary tuberculosis. Thus, the use of fluoroquinolone in treating tuberculosis is getting more pronounced, understanding the premise of DNA Gyrase interaction and resistance is becoming more vital<sup>[3,5]</sup>.

Based on CoMFA, along with CoMSIA strategies determining 3D-QSAR methods for the SAR of fluoroquinolones compounds are to be considered. On the basis of 3D-QSAR, noteworthy information can be known for further structure-based drug design, with higher activity than the template compound, the last mentioned in exhibiting the best activity reported in the literature have been designed. Our study will ponder on giving direction for the future design of more specific and potent fluoroquinolone agonists.

### Mechanism of Action

DNA Gyrase, a tetrameric A<sub>2</sub>B<sub>2</sub> protein acts by a transient double-stranded DNA, break and co-

operating to encourage DNA replication. DNA transactions, is the sole target for quinolones in Mycobacterium tuberculosis. There are three domain structures: the Gyr B domain, the Gyr A domain and a C-terminal tail, which are the members of type II sub-family of topoisomerases determined by E.coli DNA Gyrase. The portion of GyrB of DNA Gyrase compares to the ParE sub-unit of the topoisomerase IV and to N-terminal half of human and yeast topoisomerase II, with and addition of a 170 amino acids parts near to C-terminal of GyrB. From N-terminus of GyrA, about 120 amino acids are present at the active site of tyrosines. The ATP binding site is found inside the N-terminal 400 amino acids of Gyr B and ParE. Downstream of ATPase domain is the C-terminal located to GyrB that is anticipated to for the interaction between GyrA and GyrB sub-unit A region which is found in the C-terminal tail domain of DNA Gyrase is needed for wrapping about 140 base pairs of bound G-segment DNA into right handed supercoil which forms the substrate, experiences negative supercoil<sup>[4,6]</sup>. The workflow of DNA Gyrase mechanism (Figure 1).

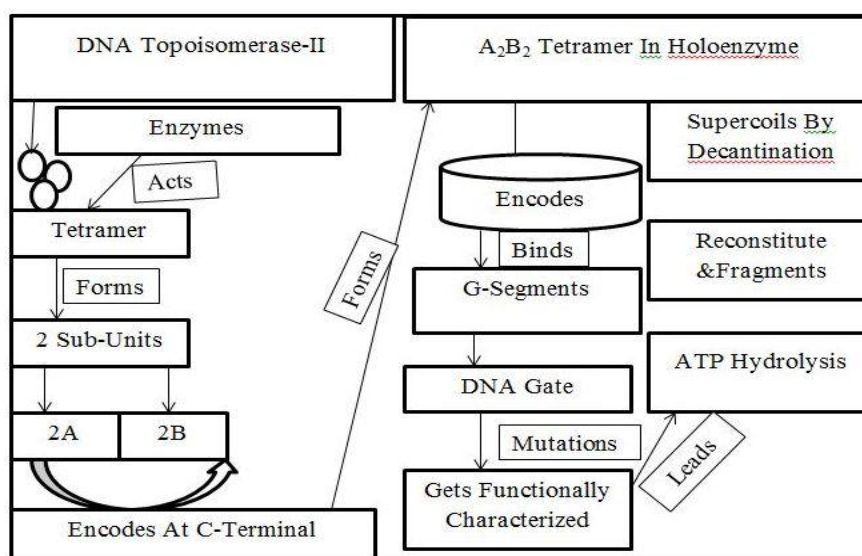


Figure 1. The workflow of DNA Gyrase.

### Materials and Methods

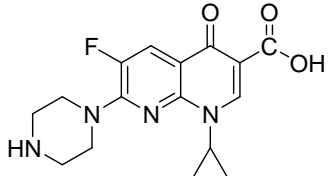
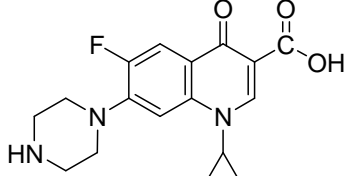
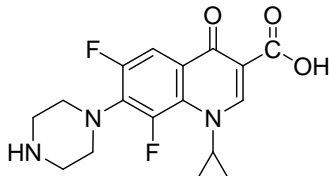
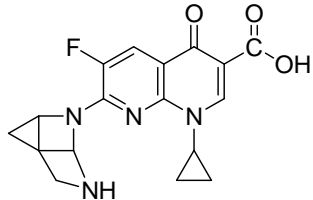
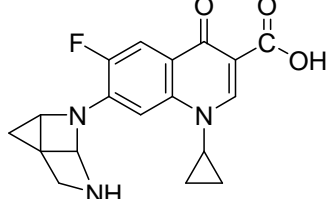
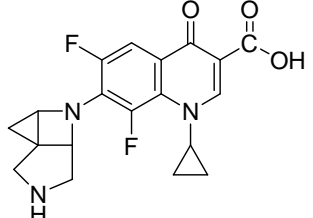
Using the software SYBYL X1.3, the molecule sketching and modelling calculations were carried out. Energy minimization was performed using Powell method with N.B. cut off 8.0 and dielectric constant 1.0 and was applied to all the compounds that were taken from the literature<sup>[7]</sup>.

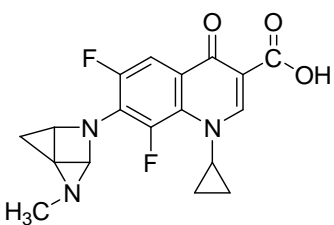
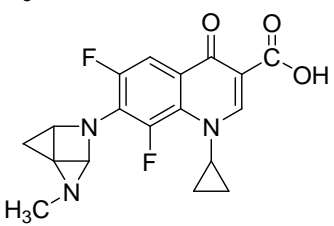
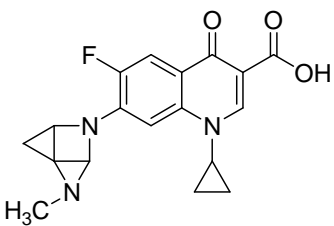
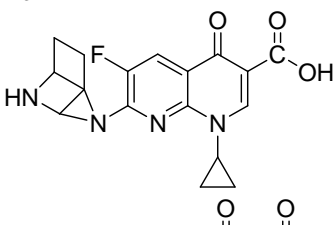
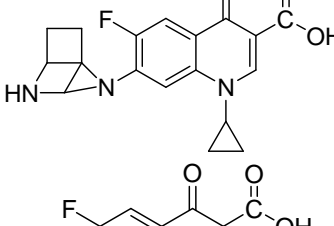
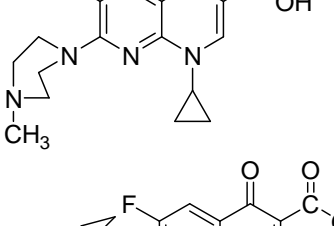
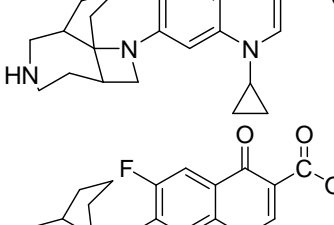
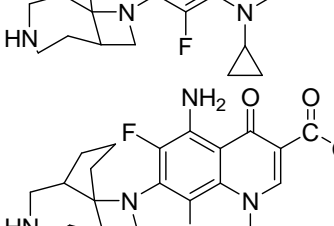
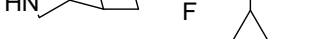
### Data Set

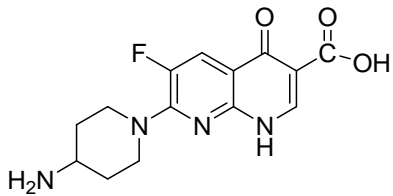
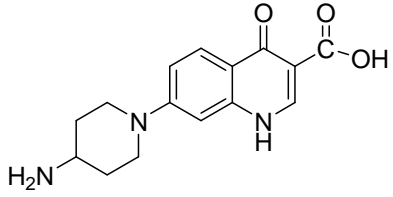
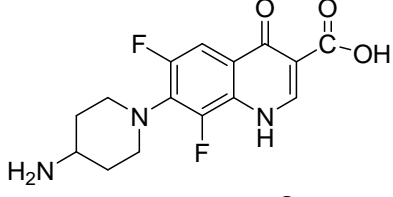
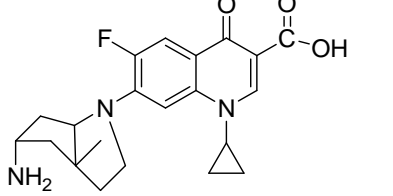
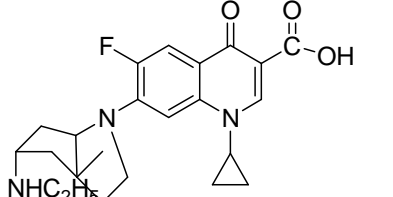
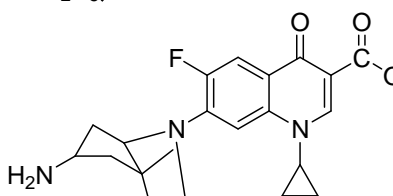
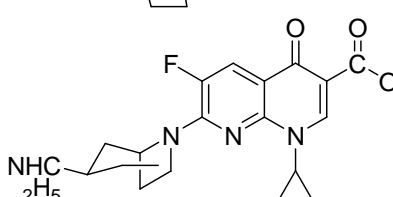
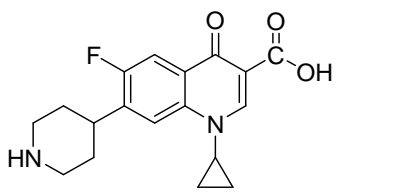
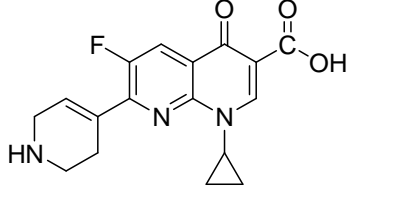
From the literature, a set of 39 molecules using the series of fluoroquinolone derivatives related to

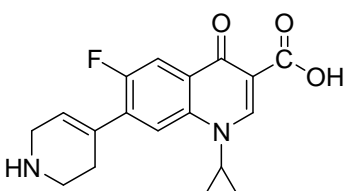
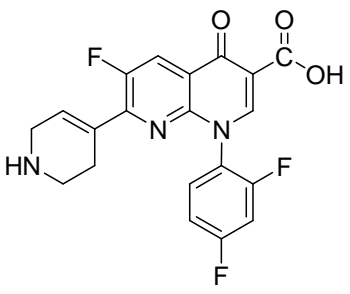
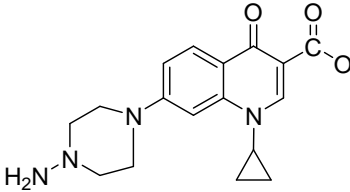
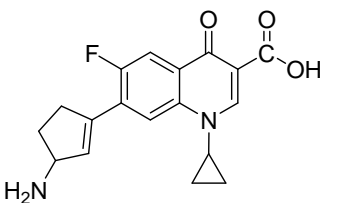
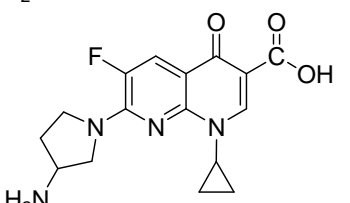
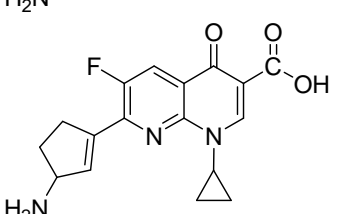
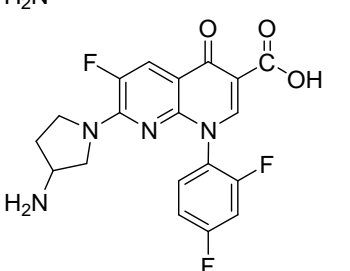
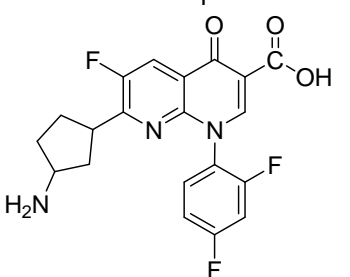
anti-TB activity was taken. The data was converted into  $pIC_{50}$  and was used as dependent variable, for PLS analysis. The data set was manually selected following 80:20 ratio formula that is 28 molecules for training set and 11 molecules for test set was selected for the development of QSAR models. Table 1 represents the molecules for the test and training sets<sup>[7,8]</sup>.

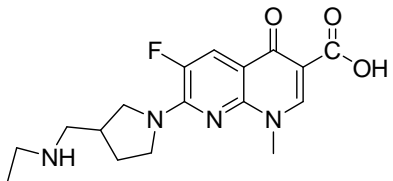
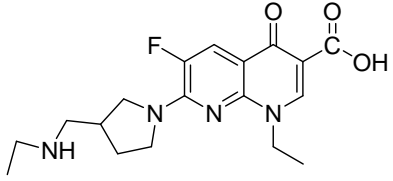
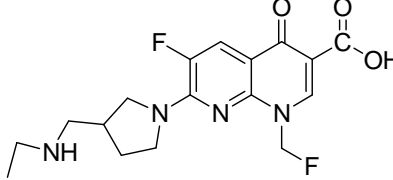
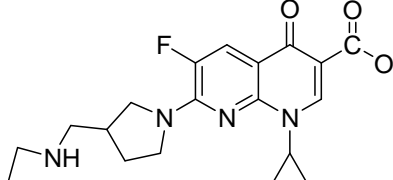
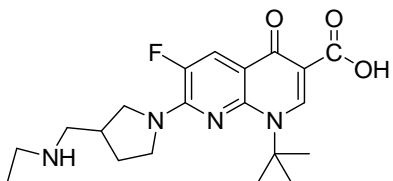
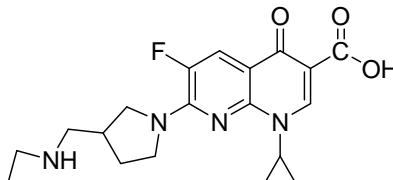
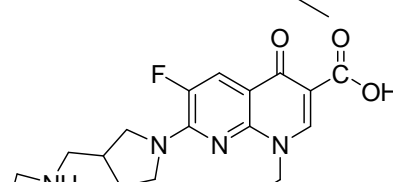
**Table 1** 2D structures of Fluoroquinolones (DNA Gyrase) targeting Mycobacterium Tuberculosis

Sr. No.	Compound	$pIC_{50}$
1		4.30
2		5.27
3		5.55
4		5.20
5		5.55
6		5.55

7		5.42
8		5.52
9		5.72
10		5.20
11		5.83
12		5.25
13		5.74
14		5.53
15		6.04

16		5.52
17		6.09
18		6.30
19		5.52
20		4.75
21		4.75
22		5.20
23		5.42
24		6.04

25		5.42
26		5.30
27		5.58
28		5.55
29		5.52
30		5.42
31		5.52
32		5.20

33		5.12
34		5.53
35		5.12
36		5.85
37		5.20
38		4.88
39		4.85

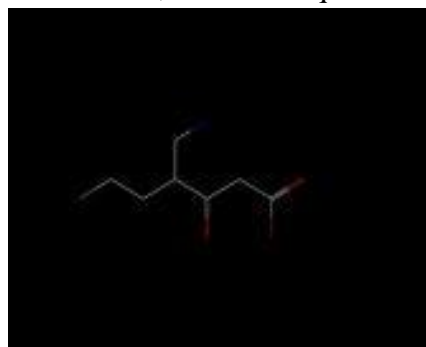
### Biological Activity

As per the literature it can be noted that the biological activity was carried on the series of fluoroquinolone derivatives using the trypanomastigote form of M.TB. The assay was performed in Dulbecco's modified eagle media. Later, the compounds were assessed with MIC values ( $\mu\text{g/ml}$ ) which was changed into  $-\log\text{MIC}$  ( $\text{pIC}_{50}$ ) that is 50% inhibitory concentration by using dependent column in QSAR model development using SYBYL X1.3 for the respective targets<sup>[7]</sup>.

### Molecular Structure Alignment

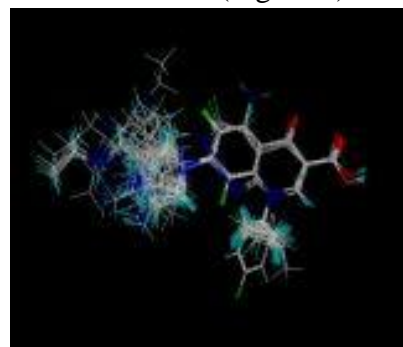
In order to obtain the finest conformers for each molecule or compound, SYBYL X1.3 software was used for the modelling of compounds and optimization parameters. Using the Tripos Force Field with 1000 interactions all structures of the compounds were preliminary subjected into geometric optimization. Gasteiger-Huckel technique was used to calculate the partial atomic charges, with energy gradient plot of 0.05 kcal/mol  $\text{\AA}^{\circ}$ . Hence, using this strategy the lowest energy conformer number 17 was chosen as template structure for the alignment of the data

sets. It is rightly known, that molecular alignment technique is considered to be one of the most important step for the development of CoMFA and CoMSIA models. Hence, the technique was



(A)

performed using distil arrangement method. Thus, rigid-body fit was used, where the remaining compounds were super-imposed on each other in SYBYLX1.3<sup>[7,8]</sup>. (Figure 2).



(B)

**Figure 2** Molecular alignment. (A) Common structure retrieved from compound 17; (B) Alignment of the compounds in the training set.

### CoMFA Method

The CoMFA method is commonly used to define the steric and electrostatic fields. Using the SYBYL X1.3 the procedure was carried out. Both fields were calculated at each lattice point with a grid spacing of 2.0 Å using sp<sup>3</sup> hybridized carbon molecule with +1 charge acting as a probe with Van Der Waals radius of 1.52 Å and a charge of +1.00. Finally, column filtering was done by setting the filters to 1.0 and 2.0 kcal/mol latter, used as a optimal parameters of this model<sup>[8,9]</sup>.

### CoMSIA Method

The CoMSIA method is similar to CoMFA in respect to the descriptors around aligned molecules. Three other fields (Hydrophobic, Hydrogen Bond Acceptor and Donor) were calculated as the same setting utilized in CoMFA calculations. Most imperatively, the Gaussian function is used to measure the distance between test molecule and each molecule atom<sup>[8,9]</sup>.

### PLS Analysis

The Partial Least Square Analysis (PLS) was carried out to determine the ideal number of components. The cross validated co-efficient  $q^2$ , acts as an internal statistical index of predictive power, was obtained. Thus, to predict the real predictive ability of the respective model derivatives by training set, biological activities of the test sets were predicted. The boot strapping by keeping 100 runs with column filtering of 2.0

kcal/mol was performed by generating new data sets from current data sets<sup>[8,9]</sup>. The quality of external prediction was reported utilizing standard error of estimation ( $R^2$ ),  $Q^2$  and  $R^2$  was calculated using the equation:

$$r_{\text{pred}}^2 = \text{SD-Press}/\text{SD}$$

where, SD = sum of square deviation between the biological activity of molecules in test set and mean of biological activity of training set.

PRESS= sum of square deviations between predicted and actual activity values for every molecule in the test set.

## Result and Discussion

### CoMFA and CoMSIA Outcome

The 3d-QSAR models were developed using the training set of 28 compounds and test set of 11 compounds. The statistical parameters related with CoMFA and CoMSIA models (Table 1). Subsequently, different alignment strategies can lead to distinctive statistical values in the developed QSAR models. The leading CoMFA and CoMSIA models were produced using a Partial Least Square (PLS) analysis, which produced cross-validated co-efficient ( $q^2$ ). When a cross-validation co-efficients,  $q^2 > 0.5$  was used, the QSAR model demonstrated statistical significance.

In table 2, two descriptor fields in CoMFA form the combination models, steric and electrostatic



fields. The CoMSIA models with combination of five descriptor fields, including steric, electrostatic, hydrophobic, hydrogen bond donor and acceptor were developed to create the optimal 3D QSAR models, yet over-fitting appeared to happen for few models (those with a large number of components). Table 2, it can be noted that the developed models (CoMFA and CoMSIA) show high  $q^2$  (0.644, 0.646),  $r^2$  (0.985, 0.993), and F-values (177.43, 193.55) along with a low standard error of estimate (SEE) (0.396, 0.287) and suitable number of components (6) which demonstrated

good co-efficient ( $r^2_{\text{pred}}$ ) including their corresponding test set molecules. The produced CoMFA and CoMSIA models with maximum external predictive ability ( $r^2_{\text{pred}}$  : 0.985, 0.977), were considered the best models. Figure 2, the actual predicted  $\text{pIC}_{50}$  values of test and training sets for CoMFA and CoMSIA are noted. The CoMFA and CoMSIA models possess a good fit with the clear diagonal line. Both the models too displayed satisfactory results throughout test and training sets.

**Table 2:** Statistical parameters of the CoMFA and CoMSIA models

Parameter	CoMFA	CoMSIA
$q^2$	0.644	0.646
$r^2_{\text{ncv}}$	0.985	0.993
$r^2_{\text{cv}}$	0.622	0.628
$r^2_{\text{bs}}$	0.990	0.978
No. of components	6	6
F-values	177.45	193.55
SEE	0.396	0.287
$r^2_{\text{pred}}$	0.985	0.977
Field Contribution	-	-
Steric	0.449	0.216
Electrostatic	0.501	0.502
Hydrophobic	-	0.426
Hydrophobic Donor	-	0.606
Hydrophobic Acceptor	-	0.423

Leave-one-out cross-validated correlation co-efficient ( $q^2$ ), noncross-validated correlation co-efficient ( $r^2$ ), standard error of estimate (SEE), Fischer test values (F), steric field (S), electrostatic field (E), hydrophobic field (H), hydrogen bond donor (D), hydrogen bond acceptor (A).

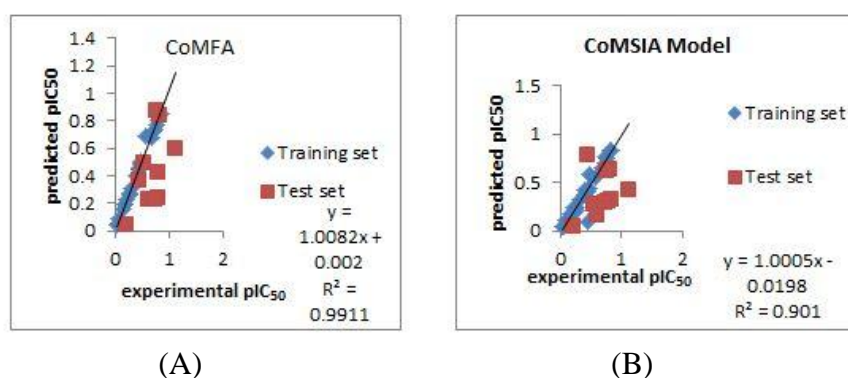


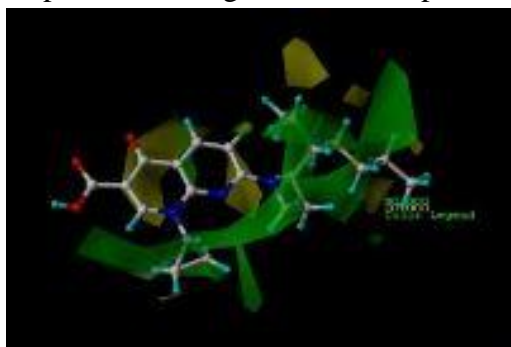
**Figure 3** Plots of Actual versus predicted  $\text{pIC}_{50}$  values, for the training set and test set compounds, for CoMFA (A) and CoMSIA (B) models.

### CoMFA Interpretation

From the contour maps, the analysis of CoMFA contour maps divulge that there is yellow polyhedron at the ortho position of the structure. This signifies that bulky group is favoured. At  $C_7$

position of 4-oxoquinolone-3-carboxylic acid, as per the literature, heterocyclic scaffold of fluoroquinolone analogues were needed for an improvement of anti-TB properties. At meta position the aromatic amines are attached between

fluorine and methoxy group are present at steric and electrostatic region. As a result, amines are favourable and may increase its activity. The benzene ring connected to three membered ring structure may increase its activity because of Nitrogen atom in the fluorine ring. Closer to it is a big green polyhedrons which signifies less bulkier groups to enhance its activity. A blue polyhedron at  $R_2$  position of the ring structure, determines that increases positive charge and is expected to

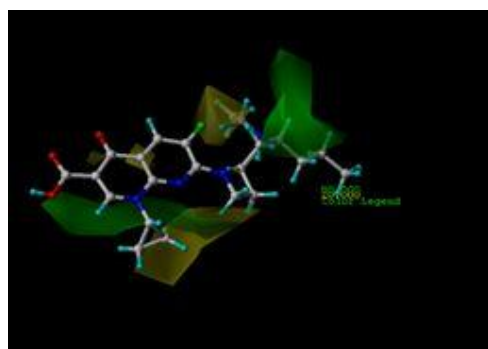


(A)

**Figure 3.** CoMFA contour maps displayed with potent compound, 17. (A) CoMFA steric contour map (green, favoured; yellow, disfavoured); (B) CoMFA electrostatic contour map (blue, electropositive favoured; red, electronegative favoured).

#### CoMSIA Interpretation

From the contour maps, the analysis of steric and electrostatic contour maps of CoMSIA models were similar to CoMFA contour maps. However, yellow colour possess steric field above benzene ring and indicates less substituents. Whereas, green colour favours bulky substituents. In case of red colour indicating electrostatic region near benzene rings shows that electron withdrawing group is required at this position. Moreover, at hydrophobic interaction indicates white colour that benzene ring is active and contributing in lipophilicity and in yellow colour near



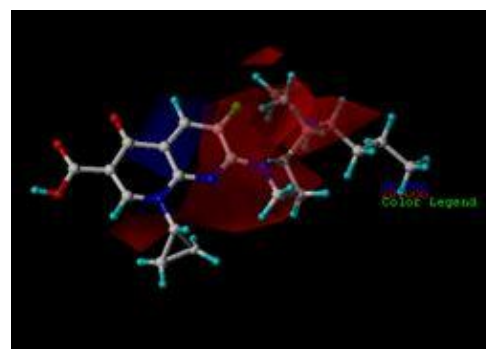
(A)

improve its activity. Furthermore, the good molecules have electronegative halogen substitutes of fluorine instead of H compound in this position. This region increases its affinity by electron withdrawing groups like aromatic amines and methoxy groups support this fact. Hence, more clear regions are seen with separate analysis of steric and electrostatic contour maps in Figure 3, respectively.



(B)

hydrophobic may increase its activity. But in hydrogen bond donor, cyan present at  $R_1$  position signifies unfavourable region as it covers half of its part which decrease its activity. Whereas, in hydrogen bond acceptor the red colour indicates disfavoured region according to group attach to methoxy group. The magenta colour close to aromatic amines may increase its activity at favourable region and thereby, favour biological activity. Hence, more clear regions are seen with separate analysis of steric, electrostatic, hydrophobic, hydrogen bond donor and acceptor contour maps in Figure 4, respectively.



(B)

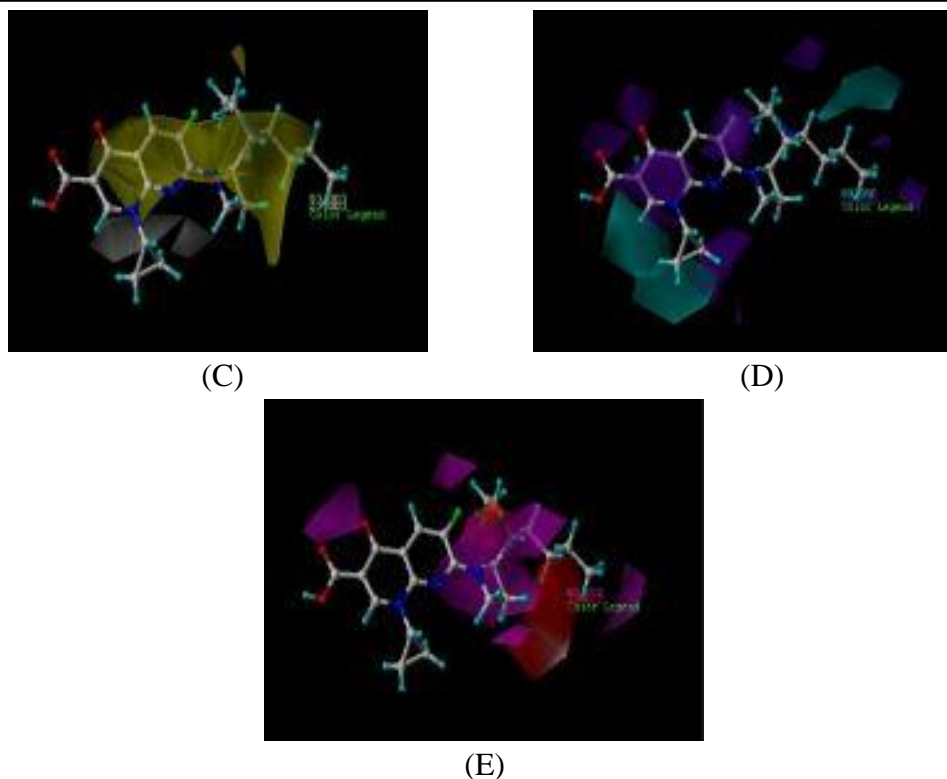


**Figure 4.** CoMSIA contour maps displayed with potent compound, **17**. (A) CoMSIA steric contour map (green, flavoured; yellow, disfavoured); (B) CoMSIA electrostatic contour map (blue, electropositive favoured; red, electronegative favoured); (C) CoMSIA hydrophobic contour map (yellow, favoured; white disfavoured); (D) CoMSIA hydrogen donor contour map (cyan, favoured; purple, disfavoured); (E) CoMSIA hydrogen acceptor contour map (magenta, favoured; red, disfavoured).

### Conclusion

In this paper, 3D-QSAR studies were carried out to examine the structural requirements for the betterment of fluoroquinolone derivative's potency as DNA Gyrase agonists. The developed CoMFA and CoMSIA models were both arithmetically significant, with high external prediction characteristics, indicating that the models can be utilized to effectively predict the compound activity. Using the various parameters and generated contour maps, the structure-activity-relationship was studied. Based on the information obtained from several contour maps, various new compounds can be derived and further can be used for model generation. By putting into a nut shell that this may be helpful for the further improvement of new DNAGyrase agonists, in the design and screening of new high-activity compounds. Figure 5 displays the core structure of compound number 17.

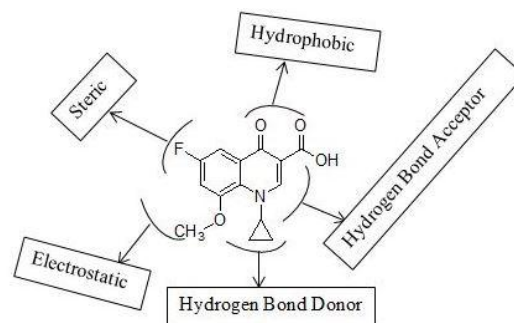


**Figure 5** Diagram of structure-activity relationship based on core structure of compound number 17.

### References

1. Adeniji SE, Uba S, Uzairu A. Quantitative structure-activity relationship and molecular docking of 4-Alkoxy-Cinnamic analogues as anti-mycobacterium tuberculosis. Journal of King Saud University.
2. Evaluation of gyrase B as a drug target in Mycobacterium tuberculosis.

3. Mycobacterium tuberculosis DNA Gyrase: Interaction with Quinolones and Correlation with Antimycobacterial Drug Activity.
4. Functional Analysis of DNA Gyrase Mutant Enzymes Carrying Mutations at Position 88 in the A Subunit Found in Clinical Strains of Mycobacterium tuberculosis Resistant to Fluoroquinolones.
5. Fluoroquinolone interactions with Mycobacterium tuberculosis gyrase: Enhancing drug activity against wild-type and resistant gyrase.
6. Functional Analysis of DNA Gyrase Mutant Enzymes Carrying Mutations at Position 88 in the A Subunit Found in Clinical Strains of Mycobacterium tuberculosis Resistant to Fluoroquinolones.
7. 2D-QSAR Study of Fluoroquinolone Derivatives: An Approach to Design Anti-tubercular Agents.
8. Masand VH, Jawarkar RD, Mahajan DT, Hadda TB, Sheikh J, Patil KN. QSAR and CoMFA studies of biphenyl analogs of the anti-tuberculosis drug (6S)-2-nitro-6-{{4-(trifluoromethoxy)benzyl}oxy}-6,7-dihydro-5H-imidazo [2,1-b][1,3]oxazine (PA-824). Medicinal Chemistry Research. 2012 Sep;21(9):2624–9.
9. Zhao X, Chen M, Huang B, Ji H, Yuan M. Comparative Molecular Field Analysis (CoMFA) and Comparative Molecular Similarity Indices Analysis (CoMSIA) Studies on  $\alpha$ 1A-Adrenergic Receptor Antagonists Based on Pharmacophore Molecular Alignment.